AMERICAN SOCIETY FOR MICROBIOLOGY | mBio®

RESEARCH ARTICLE
Host-Microbe Biology

Dynamics of *Mycobacterium tuberculosis* Ag85B Revealed by a Sensitive Enzyme-Linked Immunosorbent Assay

Joel D. Ernst,[a,b]* Amber Cornelius,[b] Miriam Bolz[b]*

[a]Division of Experimental Medicine, University of California, San Francisco, San Francisco, California, USA
[b]Division of Infectious Diseases and Immunology, Department of Medicine, New York University School of Medicine, New York, New York, USA

ABSTRACT Secretion of specific proteins contributes to pathogenesis and immune responses in tuberculosis and other bacterial infections, yet the kinetics of protein secretion and fate of secreted proteins *in vivo* are poorly understood. We generated new monoclonal antibodies that recognize the *Mycobacterium tuberculosis* secreted protein Ag85B and used them to establish and characterize a sensitive enzyme-linked immunosorbent assay (ELISA) to quantitate Ag85B in samples generated *in vitro* and *in vivo*. We found that nutritional or culture conditions had little impact on the secretion of Ag85B and that there is considerable variation in Ag85B secretion by distinct strains in the *M. tuberculosis* complex: compared with the commonly used H37Rv strain (lineage 4), *Mycobacterium africanum* (lineage 6) secretes less Ag85B, and two strains from lineage 2 secrete more Ag85B. We also used the ELISA to determine that the rate of secretion of Ag85B is 10- to 100-fold lower than that of proteins secreted by Gram-negative and Gram-positive bacteria, respectively. ELISA quantitation of Ag85B in lung homogenates of *M. tuberculosis* H37Rv-infected mice revealed that although Ag85B accumulates in the lungs as the bacterial population expands, the amount of Ag85B per bacterium decreases nearly 10,000-fold at later stages of infection, coincident with the development of T cell responses and arrest of bacterial population growth. These results indicate that bacterial protein secretion *in vivo* is dynamic and regulated, and quantitation of secreted bacterial proteins can contribute to the understanding of pathogenesis and immunity in tuberculosis and other infections.

IMPORTANCE Bacterial protein secretion contributes to host-pathogen interactions, yet the process and consequences of bacterial protein secretion during infection are poorly understood. We developed a sensitive ELISA to quantitate a protein (termed Ag85B) secreted by *M. tuberculosis* and used it to find that Ag85B secretion occurs with slower kinetics than for proteins secreted by Gram-positive and Gram-negative bacteria and that accumulation of Ag85B in the lungs is markedly regulated as a function of the bacterial population density. Our results demonstrate that quantitation of bacterial proteins during infection can reveal novel insights into host-pathogen interactions.

KEYWORDS Ag85B, ELISA, bacterial antigen, bacterial protein secretion, monoclonal antibodies, tuberculosis

Mycobacterium tuberculosis employs secretion of specific proteins (estimated to include up to ~25% of the bacterial proteome [1]) to survive, interact with host targets during infection (2, 3), manipulate its intracellular niche (2–7), and induce protective and pathogenic immune responses (8). Among the proteins that are most abundant in *M. tuberculosis* culture supernatants are members of a family of three closely related proteins, the antigen 85 (Ag85) complex, consisting of Ag85A, Ag85B, and Ag85C (9). All three of these proteins exhibit enzymatic activity as mycolyl

Citation Ernst JD, Cornelius A, Bolz M. 2019. Dynamics of *Mycobacterium tuberculosis* Ag85B revealed by a sensitive enzyme-linked immunosorbent assay. mBio 10:e00611-19. https://doi.org/10.1128/mBio.00611-19.

Editor Alan Sher, National Institute of Allergy and Infectious Diseases

Address correspondence to Joel D. Ernst, joel.ernst@ucsf.edu.

* Present address: Joel D. Ernst, UCSF Division of Experimental Medicine, San Francisco, California, USA; Miriam Bolz, Swiss Tropical Public Health Institute, University of Basel, Basel, Switzerland.

This article is a direct contribution from a Fellow of the American Academy of Microbiology. Solicited external reviewers: Sabine Ehrt, Weill Cornell Medical College; Paul Edelstein, Univ. of Penn. Perelman School of Medicine.

Received 8 March 2019
Accepted 14 March 2019
Published 23 April 2019

transferases, in which they catalyze transesterification reactions to synthesize trehalose monomycolate (TMM), trehalose dimycolate (TDM), and mycolated arabinogalactan (10, 11). Because of these enzymatic activities and their importance in constructing the mycobacterial envelope, Ag85A, Ag85B, and Ag85C have been considered potential drug targets for treatment of tuberculosis (TB) (10).

Due to their ability to induce adaptive CD4 and CD8 T lymphocyte responses in a broad range of vertebrate hosts, Ag85A and Ag85B have been investigated as antigens for tuberculosis vaccines and are prominent components of at least seven candidate vaccines in various stages of development (http://www.aeras.org). Quantitative assays of mRNA have revealed that the genes encoding Ag85A and Ag85B (*fbpA* and *fbpB*, respectively) are expressed at high levels by bacteria in the lungs early after aerosol infection of mice, but their mRNA expression decreases markedly after the recruitment of antigen-specific effector T cells to the lungs (12–14). Consistent with the results of bacterial RNA quantitation, CD4 T cells specific for Ag85B are activated in the lungs between 2 and 3 weeks after infection of mice, but their activation markedly decreases concurrent with decreased bacterial expression of the *fbpB* gene (12, 15).

Despite considerable knowledge of the properties of the *fbpA* and *fbpB* genes and the antigenicity of their products, there is less information on the secretion, *in vivo* expression, and trafficking of the Ag85A or Ag85B proteins. Because of interest in Ag85B as a vaccine and/or diagnostic antigen, we generated new monoclonal antibodies (mAbs) to Ag85B and used them to establish a highly sensitive and specific enzyme-linked immunosorbent assay (ELISA). We then employed the ELISA in studies of secretion and trafficking of the Ag85B protein *in vitro* and *in vivo*.

RESULTS

Generation and characterization of monoclonal antibodies to Ag85B. Monoclonal antibodies were generated, using standard methods (16), from mice immunized with purified recombinant *M. tuberculosis* Ag85B (rAg85B) expressed in *Escherichia coli*. Three mAbs, termed 710, 711, and 712, were selected for characterization. When examined by a direct ELISA using wells coated with purified rAg85A, rAg85B, or rAg85C and various concentrations of antibody, all three mAbs recognized Ag85B and yielded equivalent signals (Fig. 1A). The three mAbs also recognized Ag85A in the direct ELISA, although recognition of Ag85A required higher antibody concentrations and reached a lower maximum signal intensity than with Ag85B. mAb 710 generated a higher signal intensity and at lower antibody concentrations than with mAbs 711 and 712; the latter two mAbs also exhibited detectable binding to Ag85A when used at concentrations of $\geq$1 μg/ml (Fig. 1B). In contrast, mAbs 711 and 712 did not bind to Ag85C in the direct ELISA at any antibody concentration examined, while mAb 710 bound Ag85C at antibody concentrations as low as 0.01 μg/ml (Fig. 1C). Testing of the mAbs at a fixed concentration of 1 μg/ml on a dilution series of recombinant protein in the direct ELISA revealed that mAb 710 bound to Ag85A, Ag85B, and Ag85C at lower antigen concentrations than did mAb 711 or 712; mAbs 711 and 712 were indistinguishable in this assay. All three mAbs bound to Ag85B at lower antigen concentrations than required for binding to Ag85A or Ag85C (Fig. 1D and E). Together, these results indicate that mAbs 710, 711, and 712 preferentially recognize Ag85B, although each of the mAbs also binds Ag85A and Ab85C when these antigens are present at high concentrations.

Sandwich ELISA for quantitation of Ag85B. When the three mAbs were used in pairwise combinations, using one mAb for capture and another mAb conjugated to horseradish peroxidase (HRP) for detection of bound antigen, the highest sensitivity for detection of Ag85B was obtained when mAb 710 was used as the capture antibody (Fig. 2A). Although the differences were slight, sensitivity appeared to be greater when mAb 711 rather than mAb 712 was used as the detection antibody. Compared with Ag85B capture by mAb 710, mAb 711 capture allowed detection of bound Ag85B by mAb 710 but not by mAb 712. When mAb 712 was used for capture, mAb 710 was able to bind Ag85B, but mAb 711 was not. Together, these data indicate that the epitopes recognized by mAbs 711 and 712 overlap or may even be identical, while the epitope

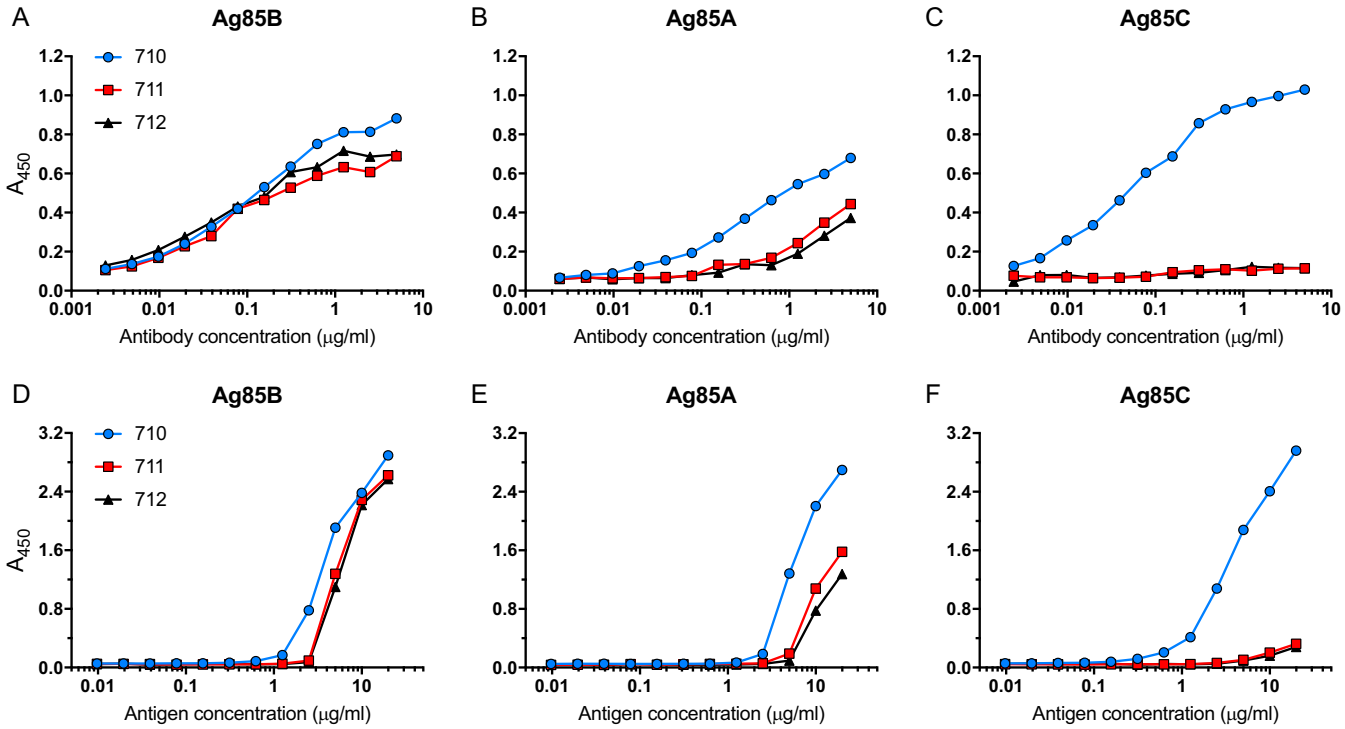

FIG 1 Recognition of Ag85A, Ag85B, and Ag85C by monoclonal antibodies 710, 711, and 712. (A to C) Wells of 96-well plates were coated with Ag85B (A), Ag85A (B), or Ag85C (C), each at 0.5 μg/ml. mAb 710, 711, or 712 was added at the indicated concentrations, and binding was detected after washing, using HRP-conjugated goat anti-mouse IgG and the TMB substrate. Data shown in panels A to C are representative of results from three independent experiments with one technical replicate per experiment per condition. (D to F) Individual wells were coated with a dilution series of Ag85B (D), Ag85A (E), or Ag85C (F), starting at 20 μg/ml. mAb 710, 711, or 712 was added at a concentration of 1 μg/ml, and binding was detected after washing, using HRP-conjugated goat anti-mouse IgG and the TMB substrate. Data in panels D to F are representative of results from two independent experiments with one technical replicate per experiment per condition.

recognized by mAb 710 is distinct from those of mAbs 711 and 712. Despite detectable binding of all three mAbs to Ag85A in the direct ELISA (Fig. 1B), none of the combinations of capture or detecting antibodies yielded a signal when Ag85A was used as the antigen in the sandwich ELISA (Fig. 2B). Likewise, despite binding of mAb 710 to Ag85C by the direct ELISA, none of the capture or detection antibody combinations resulted in a detectable signal in the sandwich ELISA when Ag85C was used as the antigen (Fig. 2C). Together, these results suggest that the epitope recognized by mAb 710 is at least partially shared by Ag85A, Ag85B, and Ag85C, while the epitope(s) recognized by mAbs 711 and 712 is more specific to Ag85B.

To confirm the specificity of the ELISA with the combination of mAbs 710 and 711 using native *M. tuberculosis* proteins, we examined culture filtrates of wild-type H37Rv and of our previously characterized Ag85B-deficient (*fbpB*-null) mutant strain of H37Rv (12). This yielded no detectable signal in the ELISA when culture filtrates of the Ag85B-deficient bacteria were examined, despite the detection of an abundant signal when wild-type culture filtrates were examined (Fig. 2D). Since the Ag85B-null bacteria retain the capacity to synthesize and secrete Ag85A and Ag85C (17), these results provide further evidence that the sandwich ELISA with mAbs 710 and 711 is highly specific for Ag85B.

The assay in this form, with mAb 710 as the capture antibody and HRP-coupled mAb 711 as the detection antibody, has been run in our laboratory >30 times to determine Ag85B content in various samples. Each assay comprised at least one standard curve with rAg85B per ELISA plate, starting at 10 ng/ml or above and including 2-fold dilutions to loss of signal (generally, ≤20 pg/ml). Three representative assay standard curves are shown in Fig. 2E. Ag85B in samples was quantitated based on either a dose-response sigmoidal regression curve or a linear regression in the linear

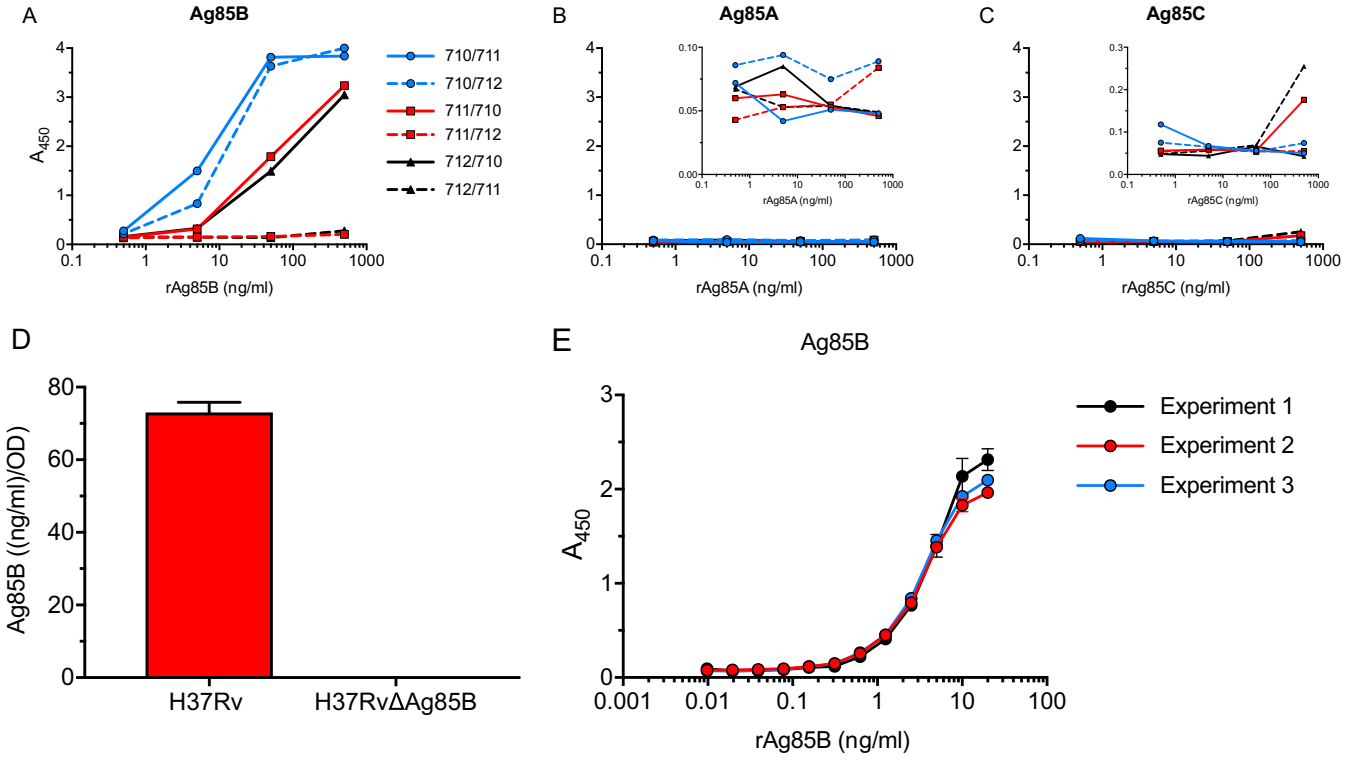

FIG 2 Characterization of the sandwich ELISA for Ag85B. Each mAb was tested as the capture antibody, with either of the remaining two mAbs (conjugated to HRP) used for detection. (A) Detection of rAg85B added to mAb-coated plates at the concentrations indicated on the *x* axis. (B) Detection of rAg85A under the same conditions as described above for panel A. The inset shows the same data on a contracted scale to reveal small differences. (C) Detection of rAg85C under the same conditions as described above for panel A. The inset shows the same data on a contracted scale to reveal small differences. (D) Specificity of the ELISA using mAb 710 for capture and HRP-conjugated mAb 711 for detection of antigen in culture filtrates of wild-type *M. tuberculosis* H37Rv or *M. tuberculosis* H37Rv with a targeted deletion of the gene encoding Ag85B. The H37Rv culture filtrate was diluted to give a signal in the linear range of the ELISA standard curve, while the H37RvΔAg85B culture filtrate was assayed undiluted. The date shown are means (bars) and standard deviations (error bars) of biological triplicate values. OD, optical density. (E) Standard curves of rAg85B in an Ag85B ELISA. Shown are curves from three independent experiments with two independent standard curves each. Shown are means (dots) and standard deviations (error bars) when large enough to depict. Data shown in panels A to C are representative of results from three independent experiments with one technical replicate per experiment per condition.

proportion of the curve (0 ng/ml to 2.5 ng/ml). With both methods, regression curves had R^2 values of >0.99. When necessary, samples were diluted for the ELISA to be in the linear range of the standard curve, and at least two technical replicates or biological replicates (when available) were run.

Carbon source effects, strain-dependent variation, and kinetics of Ag85B secretion. We used the ELISA to examine whether Ag85B secretion is governed by bacterial growth conditions. When grown in rich broth (Middlebrook 7H9 medium with 10% albumin-dextrose-catalase [ADC]), a 10-fold difference in the Tween 80 concentration (0.5% versus 0.05%) did not affect the amount of Ag85B secreted by *M. tuberculosis* H37Rv over a 24-h period (Fig. 3A). When H37Rv was grown in minimal defined medium (Sauton's medium with 0.05% Tween 80, 0.5% bovine serum albumin [BSA], and 0.05% tyloxapol) or 7H9 broth with the addition of 0.2% acetate, dextrose, or glycerol as the carbon source, the addition of acetate or glycerol did not alter Ag85B secretion, whereas 0.2% dextrose increased Ag85B secretion approximately 2-fold (Fig. 3A). These results indicate that bacterial metabolism as dictated by alternative carbon sources can affect the rate and/or amount of Ag85B secretion but that the concentration of Tween 80 had little measurable effect.

We previously reported that *Mycobacterium africanum* expresses lower levels of Ag85B than *M. tuberculosis* H37Rv, as detected by immunoblotting and by the magnitude of *in vivo* antigen-specific CD4 T cell responses (18). To verify this result and determine whether other strain-dependent variation in Ag85B secretion exists, we used the Ag85B-specific ELISA to assay culture filtrates from phylogenetically distinct bac-

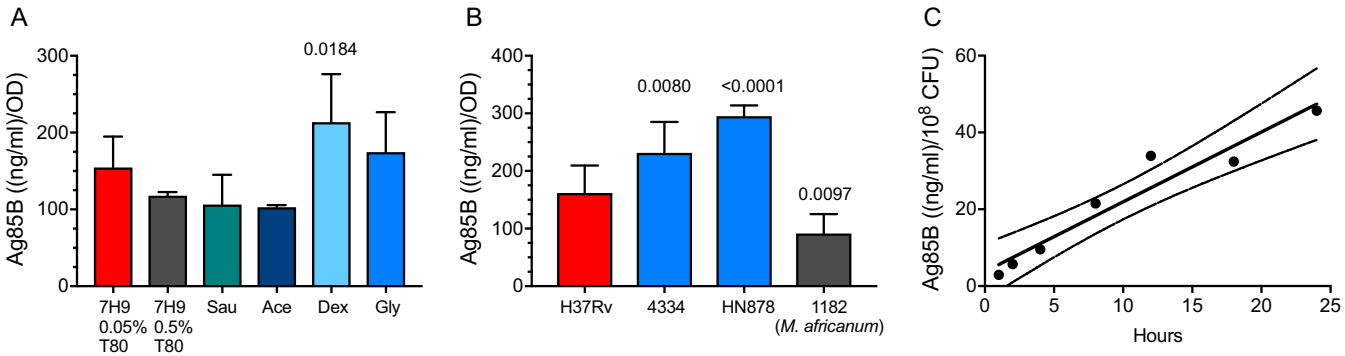

FIG 3 Effects of carbon source and *M. tuberculosis* strain, and kinetics of Ag85B secretion. (A) Effects of medium composition and carbon source on Ag85B secretion. Mid-log-phase bacteria (A_{600} = 1.0) grown in 7H9 medium were washed 5 times and then diluted 10-fold into the indicated media. After 24 h, the A_{600} was determined for each culture, and sterile filtrates were prepared for analysis by a mAb 710-711 ELISA. Results of Ag85B quantitation by the ELISA were normalized by the A_{600} of the individual culture. 7H9 0.05% T80, Middlebrook 7H9 medium with 10% ADC and 0.05% (vol/vol) Tween 80; 7H9 0.5% T80, same as above but with 0.5% Tween 80; Sau, Sauton's medium with 0.05% Tween 80; Ace, 7H9 medium with acetate; Dex, 7H9 medium with dextrose; Gly, 7H9 medium with glycerol. Show are means (bars) and standard deviations (error bars) of biological triplicate values. Statistical comparison was done using one-way analysis of variance (ANOVA); the adjusted *P* value after Dunnett's posttest for multiple comparisons was applied and is shown for the effect of dextrose. Other effects were not significant after adjusting for multiple comparisons. (B) Mycobacterial strain-dependent variation of Ag85B secretion. Mid-log-phase cultures were collected, and the bacteria of each strain were washed and resuspended in fresh 7H9 broth. After 24 h, the bacteria were pelleted by centrifugation, and Ag85B in culture filtrates was quantitated by an ELISA. Show are means (bars) and standard deviations (error bars) of biological triplicate values. The adjusted *P* values shown are for comparison of each strain with H37Rv and were determined by one-way ANOVA with Dunnett's posttest. (C) Kinetics of Ag85B secretion by *M. tuberculosis* H37Rv. Mid-log-phase growing H37Rv cells were washed, added to fresh 7H9 medium at 1×10^8 CFU/ml, and incubated for 24 h. Individual cultures were sampled at the designated time points, and culture filtrates were assayed by an ELISA. Statistical analysis by linear regression was performed using Prism 7. Dashed lines indicate 95% confidence intervals. Panel A shows data from one representative of three independent experiments. Panels B and C show data from experiments done once each.

terial isolates. This confirmed that *M. africanum* secretes significantly smaller quantities of Ag85B than *M. tuberculosis* H37Rv (Fig. 3B). We also found that two distinct isolates of *M. tuberculosis* from lineage 2 (which includes the Beijing family) secrete significantly larger quantities of Ag85B than H37Rv (Fig. 3B). These results indicate substantial variation in the secretion of Ag85B, according to the bacterial strain, possibly in a lineage-dependent manner.

To further characterize the properties of Ag85B, we determined the kinetics of its secretion by *M. tuberculosis* H37Rv. Washed mid-log-phase bacteria were suspended in fresh 7H9 medium at 10^8 CFU/ml, and culture filtrates were harvested at multiple intervals and assayed by an ELISA. The rate of accumulation of Ag85B in culture filtrates was linear (r^2 = 0.93) during the 24-h period of sampling, at 1.8 ± 0.2 ng/ml/h (Fig. 3C). Since the mature Ag85B protein has a molecular weight of 34,580, this is equivalent to 52 fmol per 10^8 CFU per h, or approximately 300 molecules secreted per bacterial cell per h.

Cell-free Ag85B during infection *in vivo* and *in vitro*. Despite their biological activity and roles in pathogenesis and immune responses, little is known of the *in vivo* fate or distribution of secreted *M. tuberculosis* proteins, especially during infection. Therefore, we examined supernatants of lung homogenates obtained at various intervals after infecting C57BL/6 mice with *M. tuberculosis* H37Rv by aerosol. We found that Ag85B was detectable in lung homogenate supernatants in some, but not all, mice as early as 4 to 8 days postinfection, followed by a progressive increase between 14 and 21 days postinfection (Fig. 4A). Since the samples for the assay were taken during the progressive growth phase of the bacteria in the lungs, the quantity of Ag85B detected is a function of the amount secreted by each bacterium and the number of bacteria, which increases progressively until approximately 21 days postinfection (19). Therefore, we normalized the concentration of Ag85B in lung homogenates by the number of bacteria present in the lungs at each time point sampled. This revealed a progressive decrease in the amount of Ag85B relative to the bacterial population size, commencing at between 8 and 11 days postinfection (Fig. 4B). This result is consistent with results of Ag85B RNA quantitation in bacterial populations in the lungs of immunocompetent mice (12–14) and with results of studies indicating that activation of Ag85B-specific CD4

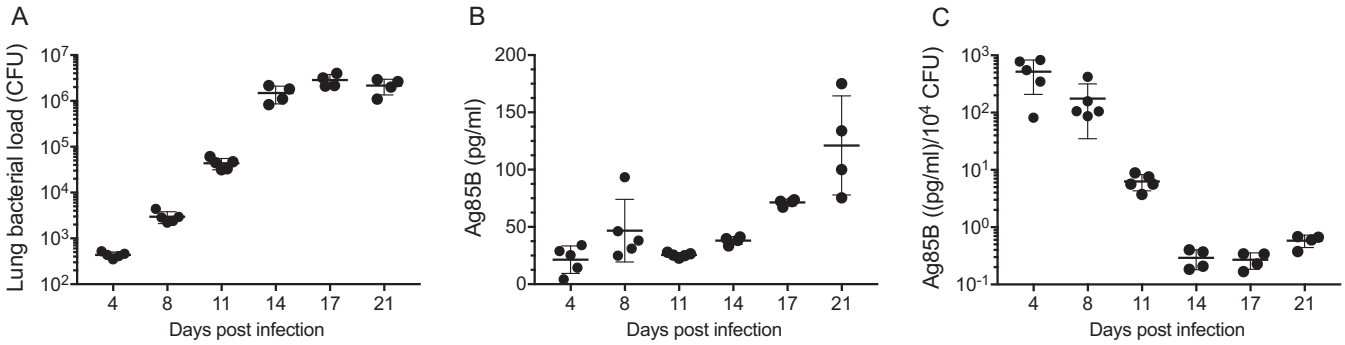

FIG 4 Quantitation of Ag85B in supernatants of lung homogenates from mice infected with *M. tuberculosis* H37Rv. (A) *M. tuberculosis* CFU in the lung samples used for assays in panel B. (B) Ag85B concentrations quantitated by an ELISA in lung homogenate supernatants; (C) Ag85B concentrations as described above for panel B, normalized by the number of bacteria (CFU) in the same lung homogenates. Shown are individual data points (means ± standard deviations). This experiment was done once.

T cells *in vivo* decreases markedly after 2 to 3 weeks of infection, due to the limited availability of the antigen (12, 15).

There are several potential sources of free Ag85B in the lungs. First is that some of the bacteria may be extracellular and may secrete Ag85B directly to the intercellular spaces in lung tissues. Second is that, as we have recently reported, Ag85B and other secreted mycobacterial proteins can be exported from infected cells by a vesicular transport pathway (20, 21). A third potential mechanism is the release of Ag85B associated with bacterial membrane vesicles (22) and/or exosomes shed by infected cells (23, 24). A fourth possible mechanism is that Ag85B synthesized by intracellular bacteria may be released from dying infected cells. We investigated the latter possibility using bone marrow-derived dendritic cells (BMDC) infected with *M. tuberculosis* H37Rv. Under conditions of the multiplicities of infection, bacterial strain, and time points used, we observed a range of loss of cell viability as reflected by a luminescence assay of ATP in cell lysates, after harvesting conditioned medium for the assay of Ag85B by an ELISA. This revealed a correlation between the loss of cell viability and the quantity of Ag85B in conditioned medium ($r^2 = 0.5777$; $P < 0.0001$) (Fig. 5), indicating that Ag85B can be released from dead and/or dying infected cells in a form that remains detectable by the ELISA. This suggests that death of infected cells can be a source of the Ag85B detected in cell-free homogenates of the lungs of infected mice, as shown in Fig. 4.

DISCUSSION

In this work, we developed three new murine monoclonal antibodies by immunizing mice with recombinant *M. tuberculosis* Ag85B and used them to develop a sensitive and

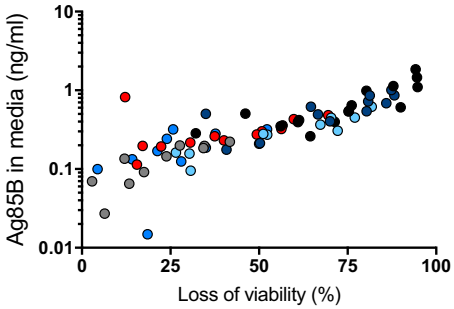

FIG 5 Death of *M. tuberculosis*-infected primary dendritic cells releases Ag85B. Bone marrow-derived dendritic cells were infected with *M. tuberculosis* H37Rv at different multiplicities of infection (1, 2, 4, and 8). At the designated time points (gray dots, 12 h; medium blue dots, 16 h; red dots, 24 h; light blue dots, 36 h; dark blue dots, 48 h), medium was removed for quantitation by an ELISA, and dendritic cell viability was assessed by a luminescence assay of ATP of cell lysates. Results of the two assays on a given sample were plotted as a data point, and Pearson correlation was determined for the whole data set. Shown are representative results of two similar experiments.

specific ELISA for quantitation of Ag85B in various biological samples. We found that, compared with the H37Rv strain of *M. tuberculosis* complex lineage 4, two isolates of lineage 2 secreted large quantities, while a lineage 6 (*M. africanum*) isolate secreted small quantities, of Ag85B. Since Ag85B plays a role in the synthesis of trehalose dimycolate, and trehalose dimycolate is a potent proinflammatory mediator during *M. tuberculosis* infection (25–28), the results suggest that differences in Ag85B secretion may contribute to strain-dependent differences in the proinflammatory properties of distinct strains and lineages in the *M. tuberculosis* complex (29). Strain variability in secretion may also influence the frequency and magnitude of T cell responses to Ag85B, which may provide an explanation for the finding that few human subjects exhibit detectable responses to Ag85B compared with other antigens such as ESAT-6 and/or CFP-10 (30, 31). Likewise, bacterial strain-dependent variation in the secretion of Ag85B may influence the protective efficacy of TB subunit vaccines that include Ag85B: even if a vaccine generates immune responses to Ag85B, vaccination may provide little protection against infection with mycobacterial strains that express and secrete small quantities of Ag85B. In studies of subunit vaccines that include Ag85B, it may be informative to characterize Ag85B expression and secretion in isolates of *M. tuberculosis* from subjects who develop breakthrough infections despite apparently appropriate immune responses to the vaccine antigen.

We also used the ELISA to determine that the rate of secretion by *M. tuberculosis* H37Rv in broth culture is approximately 300 molecules of Ag85B per bacterial cell per h. This is 10- to 100-fold lower than the rate of translocation of *E. coli* proOmpA (4.5 mol/min) (32) or the secretion of staphylococcal toxic shock toxin (1.1×10^4 molecules/CFU/h) (33). A full understanding of the basis for this difference will require determination of the rates of protein synthesis in *M. tuberculosis* compared with those in other bacteria and characterization of the factors and mechanisms that determine the rate of protein secretion by distinct secretion systems in bacteria. Given the important roles of secreted protein virulence factors in *M. tuberculosis* and other bacterial pathogens, a better understanding of protein secretion may reveal new targets for therapeutic modulation and reduction of disease and pathogen transmission.

A third major finding in these studies is that *M. tuberculosis* Ag85B can be found in homogenized lung tissue supernatants from infected mice. This finding has several potential implications. If data from studies of human subjects provide supportive data, then detecting Ag85B in respiratory secretions may provide a rapid and economical approach to diagnosing pulmonary tuberculosis and may also be useful in monitoring responses to treatment. Another is that the presence of extracellular Ag85B in lung tissue may make Ag85B available for uptake, processing, and presentation by uninfected dendritic cells and macrophages in the lungs. Since we have reported that direct recognition of infected cells is required for optimal CD4 T cell control of intracellular *M. tuberculosis* (34), acquisition and presentation of Ag85B by uninfected cells in the lungs may provide antigen-loaded decoys for Ag85B-specific CD4 T cells that reduce the frequency of recognition of infected cells by those T cells. This is consistent with our recent finding in mouse lungs (35) and the finding in lungs of *M. tuberculosis*-infected rhesus macaques (36) that only a small fraction of the T cells in the lungs are in close contact with *M. tuberculosis*-infected cells. Our associated finding in this work that death of *M. tuberculosis*-infected host cells can be associated with the release of Ag85B to the extracellular space indicates that the presence of Ag85B (and other mycobacterial proteins) in extracellular tissue compartments in the lungs may be the consequence of secretion by extracellular bacteria, vesicular transport from infected cells (21), carriage by exosomes (37, 38), and release by dying or dead host cells. Since Ag85B (39, 40), ESAT-6 (41), and other mycobacterial proteins have been reported to act on host cells to modulate inflammation, our findings provide additional evidence for the plausibility that extracellular mycobacterial proteins contribute to the pathogenesis of TB and may be susceptible to therapeutic modulation.

MATERIALS AND METHODS

Ethics statement. All animal experiments were done in accordance with procedures approved by the New York University School of Medicine Institutional Animal Care and Use Committee (laboratory animal care protocol 150502-01), which conformed to the guidelines provided by the *Guide for the Care and Use of Laboratory Animals* of the National Institutes of Health (42).

Bacterial strains. The stocks of *M. tuberculosis* H37Rv, H37Rv::Δ*fbpB* (Ag85B null), and 4334 and *M. africanum* 1182 used in our laboratory and for these studies were previously described (19, 43–45). The *M. tuberculosis* HN878 strain was obtained from BEI Resources.

Recombinant Ag85B. RV1886c-ss.pET23b was transformed into *E. coli* BL21(DE3)/pLysS (Invitrogen) and induced with 0.8 mM isopropyl-β-D-thiogalactopyranoside (IPTG) for 4 h at 37°C. Cultures were lysed with a solution containing 50 mM Tris (pH 7.0), 150 mM NaCl, lysozyme, Benzonase, and 1 mM phenylmethylsulfonyl fluoride (PMSF) for 30 min at 22°C on an orbital shaker. The lysate was spun at 10,000 × *g* for 30 min, sterile filtered, and loaded onto an Akta fast protein liquid chromatography (FPLC) His-Trap column (GE). The column was washed with 50 mM imidazole, and recombinant protein was eluted with 250 mM imidazole. Purity was assessed by SDS-PAGE.

mAb generation and selection. BALB/c mice were immunized with purified recombinant Ag85B (100 μg/mouse for 2 injections followed by 50 μg/mouse for 2 additional injections) subcutaneously in TiterMax gold (TiterMax, Norcross, GA, USA), followed by 50 μg/mouse given intravenously 3 days before harvesting and using spleen cells in fusions with P3X63Ag8 myeloma cells. Hybridoma supernatants were screened for recognition of rAg85B-coated wells by an ELISA.

Direct ELISA for characterization of individual mAbs. Ag85A (catalog number NR-14871; BEI Resources), Ag85B (our purified recombinant), or Ag85C (catalog number NR-14858; BEI Resources) was used to coat wells at 0.5 μg/well in phosphate-buffered saline (PBS) and incubated overnight at 4°C. The plates were washed 3 times with PBS (pH 7.4) with 0.05% Tween 20 and blocked with PBS containing 1.0% BSA for 1 h. A starting concentration of 5 μg/ml of mAb 710, 711, or 712 was serially diluted, and 200 μl/well was incubated at room temperature for 2 h. Plates were washed 5 times and incubated with goat anti-mouse IgG-HRP (MP Biomedicals) for 1 h at room temperature. Plates were washed 7 times and developed with the 3,3′,5,5′-tetramethylbenzidine (TMB) substrate according to the manufacturer's instructions (BD). The reaction was stopped with 2 M sulfuric acid, and the absorbance was read at 450 nm with a Synergy H1 microplate reader (BioTek).

Mycobacterial culture filtrates. *M. tuberculosis* strains H37RV, 4334, and HN878, or *M. africanum* strain 1182, were inoculated from a 1-ml frozen stock of approximately 3×10^8 CFU/ml into 10 ml of Middlebrook 7H9 medium supplemented with 0.5% albumin, 0.2% dextrose, and 0.3 mg/100 ml catalase (termed 7H9 in the text) and grown to late log phase. The cultures were then passaged and grown once to mid-log phase. Cultures were then collected and spun at 150 × *g*. The collected supernatant was then spun at 3,750 × *g* for 5 min and washed with PBS. The pellets were then resuspended in fresh 7H9 medium and grown for 24 h. The cultures were pelleted, and the medium was sterile filtered.

Sandwich ELISA development and optimization. Individual mAbs were used at 2.5 μg/ml in 50 μl 0.05 M carbonate-bicarbonate buffer to coat wells overnight at 4°C. The plates were washed 3 times with PBS (pH 7.4) with 0.5% Tween 20 and blocked with PBS containing 1.0% BSA for 1 h. Antibodies for detection were conjugated to HRP according to the manufacturer's recommendations (Abcam). Briefly, 1 μl of the modifier was mixed with 10 μl of antibody and then added to a vial of HRP mix. The vial was incubated overnight at room temperature in the dark. After incubation, 1 μl of the quencher was added and mixed. The conjugated antibodies were diluted to 0.5 μg/ml in PBS with 1% BSA and stored in aliquots at −20°C until first use. Upon thawing, conjugated antibodies were stored at 4°C.

For ELISAs, samples were added to plates coated with the designated antibody and incubated at room temperature for 2 h, and plates were then washed 5 times. The labeled detection antibody was added, and the plates were incubated at room temperature for 1 h. Plates were washed 7 times and developed with the substrate according to the manufacturer's instructions (BD). The reaction was stopped with 2 M sulfuric acid, and the absorbance was read at 450 nm.

Sandwich ELISA application. The routine sandwich ELISA was performed according to the procedures described above, with mAb 710 as the capture antibody used to coat wells and HRP-conjugated mAb 711 used to detect bound antigen. Signal generation for the HRP reaction was done by using the TMB substrate (Thermo Scientific).

Effects of medium and carbon source. After washing in PBS, bacteria were resuspended in 6 ml of distilled water and split among 6 bottles. Ten milliliters of medium was added to the bottles. The medium used was Middlebrook 7H9 medium with 10% ADC and either 0.05% or 0.5% Tween 80 or Sauton's broth with 0.05% Tween 80, 0.5% BSA, 0.05% tyloxapol, and 0.2% (wt/vol) acetate, glycerol, or dextrose (adapted from reference 46), and bacteria were incubated for 24 h prior to preparation of culture filtrates.

Preparation of lung homogenate supernatants from *M. tuberculosis*-infected mice. C57BL/6 mice were infected by the aerosol route with ~60 CFU/mouse of *M. tuberculosis* H37Rv, lungs were harvested, and single-cell suspensions were prepared as previously described (47). After sampling the cell suspensions for determination of bacterial CFU, an aliquot of each sample was sterile filtered, and the Ag85B concentration was determined by an ELISA.

Culture, infection, and analysis of bone marrow-derived dendritic cell death and release of Ag85B. Bone marrow-derived dendritic cells (BMDC), generated as previously described (20), were seeded in 96-well tissue culture-treated plates (Corning) at 2×10^6 cells/well, rested for 2 h, infected overnight at different multiplicities of infection (1, 2, 4, and 8) with *M. tuberculosis* H37Rv, treated with amikacin (200 μg/ml for 40 min) in BMDC medium (RPMI 1640 supplemented with 10% heat-inactivated fetal bovine serum [FBS], 2 mM L-glutamine, 1 mM sodium pyruvate, 1× β-mercaptoethanol, 10 mM

HEPES, and 12 ng/ml recombinant mouse granulocyte-macrophage colony-stimulating factor [GM-CSF]), washed three times in PBS, and further cultured in fresh BMDC medium. Conditioned medium (CM) was harvested 16, 24, 34, and 48 h later and sterile filtered, and Ag85B in CM was quantified by a sandwich ELISA. At each harvest time point, infected BMDC were assayed for cell death by using CellTiter-Glo (Promega) according to the manufacturer's instructions, and the signal was read as luminescence with a Synergy H1 microplate reader (BioTek). For each harvest time point, the signal from uninfected cells was considered 100% viability for determination of loss of viability of infected cells.

Statistical analyses. All statistical analyses were performed using Prism 7 (GraphPad). The specific tests used for data analysis are specified in the individual figure legends.

ACKNOWLEDGMENTS

We thank Smita Srivastava for her contributions to the initial stages of this project.

This work was supported by funds from the National Institutes of Health (R01 AI051242 and R01 AI124471 [J.D.E.]) and the Swiss National Science Foundation (P2BSP3-165349 [M.B.]).

REFERENCES

1. Miller BK, Zulauf KE, Braunstein M. 2017. The Sec pathways and exportomes of Mycobacterium tuberculosis. Microbiol Spectr 5:TBTB2-0013-2016. https://doi.org/10.1128/microbiolspec.TBTB2-0013-2016.
2. Mehra A, Zahra A, Thompson V, Sirisaengtaksin N, Wells A, Porto M, Koster S, Penberthy K, Kubota Y, Dricot A, Rogan D, Vidal M, Hill DE, Bean AJ, Philips JA. 2013. Mycobacterium tuberculosis type VII secreted effector EsxH targets host ESCRT to impair trafficking. PLoS Pathog 9:e1003734. https://doi.org/10.1371/journal.ppat.1003734.
3. Penn BH, Netter Z, Johnson JR, Von Dollen J, Jang GM, Johnson T, Ohol YM, Maher C, Bell SL, Geiger K, Golovkine G, Du X, Choi A, Parry T, Mohapatra BC, Storck MD, Band H, Chen C, Jager S, Shales M, Portnoy DA, Hernandez R, Coscoy L, Cox JS, Krogan NJ. 2018. An Mtb-human protein-protein interaction map identifies a switch between host antiviral and antibacterial responses. Mol Cell 71:637.e5–648.e5. https://doi.org/10.1016/j.molcel.2018.07.010.
4. Manzanillo PS, Shiloh MU, Portnoy DA, Cox JS. 2012. Mycobacterium tuberculosis activates the DNA-dependent cytosolic surveillance pathway within macrophages. Cell Host Microbe 11:469–480. https://doi.org/10.1016/j.chom.2012.03.007.
5. Simeone R, Bobard A, Lippmann J, Bitter W, Majlessi L, Brosch R, Enninga J. 2012. Phagosomal rupture by Mycobacterium tuberculosis results in toxicity and host cell death. PLoS Pathog 8:e1002507. https://doi.org/10.1371/journal.ppat.1002507.
6. Simeone R, Sayes F, Song O, Groschel MI, Brodin P, Brosch R, Majlessi L. 2015. Cytosolic access of Mycobacterium tuberculosis: critical impact of phagosomal acidification control and demonstration of occurrence in vivo. PLoS Pathog 11:e1004650. https://doi.org/10.1371/journal.ppat.1004650.
7. van der Wel N, Hava D, Houben D, Fluitsma D, van Zon M, Pierson J, Brenner M, Peters PJ. 2007. M. tuberculosis and M. leprae translocate from the phagolysosome to the cytosol in myeloid cells. Cell 129:1287–1298. https://doi.org/10.1016/j.cell.2007.05.059.
8. Woodworth JS, Cohen SB, Moguche AO, Plumlee CR, Agger EM, Urdahl KB, Andersen P. 2017. Subunit vaccine H56/CAF01 induces a population of circulating CD4 T cells that traffic into the Mycobacterium tuberculosis-infected lung. Mucosal Immunol 10:555–564. https://doi.org/10.1038/mi.2016.70.
9. Wiker HG, Harboe M. 1992. The antigen 85 complex: a major secretion product of Mycobacterium tuberculosis. Microbiol Rev 56:648–661.
10. Backus KM, Dolan MA, Barry CS, Joe M, McPhie P, Boshoff HI, Lowary TL, Davis BG, Barry CE, III. 2014. The three Mycobacterium tuberculosis antigen 85 isoforms have unique substrates and activities determined by non-active site regions. J Biol Chem 289:25041–25053. https://doi.org/10.1074/jbc.M114.581579.
11. Belisle JT, Vissa VD, Sievert T, Takayama K, Brennan PJ, Besra GS. 1997. Role of the major antigen of Mycobacterium tuberculosis in cell wall biogenesis. Science 276:1420–1422. https://doi.org/10.1126/science.276.5317.1420.
12. Bold TD, Banaei N, Wolf AJ, Ernst JD. 2011. Suboptimal activation of antigen-specific CD4+ effector cells enables persistence of M. tuberculosis in vivo. PLoS Pathog 7:e1002063. https://doi.org/10.1371/journal.ppat.1002063.
13. Rogerson BJ, Jung YJ, LaCourse R, Ryan L, Enright N, North RJ. 2006. Expression levels of Mycobacterium tuberculosis antigen-encoding genes versus production levels of antigen-specific T cells during stationary level lung infection in mice. Immunology 118:195–201. https://doi.org/10.1111/j.1365-2567.2006.02355.x.
14. Shi L, North R, Gennaro ML. 2004. Effect of growth state on transcription levels of genes encoding major secreted antigens of Mycobacterium tuberculosis in the mouse lung. Infect Immun 72:2420–2424. https://doi.org/10.1128/IAI.72.4.2420-2424.2004.
15. Moguche AO, Musvosvi M, Penn-Nicholson A, Plumlee CR, Mearns H, Geldenhuys H, Smit E, Abrahams D, Rozot V, Dintwe O, Hoff ST, Kromann I, Ruhwald M, Bang P, Larson RP, Shafiani S, Ma S, Sherman DR, Sette A, Lindestam Arlehamn CS, McKinney DM, Maecker H, Hanekom WA, Hatherill M, Andersen P, Scriba TJ, Urdahl KB. 2017. Antigen availability shapes T cell differentiation and function during tuberculosis. Cell Host Microbe 21:695.e5–706.e5. https://doi.org/10.1016/j.chom.2017.05.012.
16. Greenfield EA (ed). 2014. Antibodies: a laboratory manual. Cold Spring Harbor Laboratory Press, Cold Spring Harbor, NY.
17. Grace PS, Ernst JD. 2016. Suboptimal antigen presentation contributes to virulence of Mycobacterium tuberculosis in vivo. J Immunol 196:357–364. https://doi.org/10.4049/jimmunol.1501494.
18. Bold TD, Davis DC, Penberthy KK, Cox LM, Ernst JD, de Jong BC. 2012. Impaired fitness of Mycobacterium africanum despite secretion of ESAT-6. J Infect Dis 205:984–990. https://doi.org/10.1093/infdis/jir883.
19. Wolf AJ, Desvignes L, Linas B, Banaiee N, Tamura T, Takatsu K, Ernst JD. 2008. Initiation of the adaptive immune response to Mycobacterium tuberculosis depends on antigen production in the local lymph node, not the lungs. J Exp Med 205:105–115. https://doi.org/10.1084/jem.20071367.
20. Srivastava S, Ernst JD. 2014. Cell-to-cell transfer of M. tuberculosis antigens optimizes CD4 T cell priming. Cell Host Microbe 15:741–752. https://doi.org/10.1016/j.chom.2014.05.007.
21. Srivastava S, Grace PS, Ernst JD. 2016. Antigen export reduces antigen presentation and limits T cell control of M. tuberculosis. Cell Host Microbe 19:44–54. https://doi.org/10.1016/j.chom.2015.12.003.
22. Lee J, Kim SH, Choi DS, Lee JS, Kim DK, Go G, Park SM, Kim SH, Shin JH, Chang CL, Gho YS. 2015. Proteomic analysis of extracellular vesicles derived from Mycobacterium tuberculosis. Proteomics 15:3331–3337. https://doi.org/10.1002/pmic.201500037.
23. Giri PK, Kruh NA, Dobos KM, Schorey JS. 2010. Proteomic analysis identifies highly antigenic proteins in exosomes from M. tuberculosis-infected and culture filtrate protein-treated macrophages. Proteomics 10:3190–3202. https://doi.org/10.1002/pmic.200900840.
24. Ramachandra L, Qu Y, Wang Y, Lewis CJ, Cobb BA, Takatsu K, Boom WH, Dubyak GR, Harding CV. 2010. Mycobacterium tuberculosis synergizes with ATP to induce release of microvesicles and exosomes containing major histocompatibility complex class II molecules capable of antigen presentation. Infect Immun 78:5116–5125. https://doi.org/10.1128/IAI.01089-09.
25. Ishikawa E, Ishikawa T, Morita YS, Toyonaga K, Yamada H, Takeuchi O, Kinoshita T, Akira S, Yoshikai Y, Yamasaki S. 2009. Direct recognition of the mycobacterial glycolipid, trehalose dimycolate, by C-type lectin Mincle. J Exp Med 206:2879–2888. https://doi.org/10.1084/jem.20091750.

26. Miyake Y, Toyonaga K, Mori D, Kakuta S, Hoshino Y, Oyamada A, Yamada H, Ono K, Suyama M, Iwakura Y, Yoshikai Y, Yamasaki S. 2013. C-type lectin MCL is an FcRgamma-coupled receptor that mediates the adjuvanticity of mycobacterial cord factor. Immunity 38:1050–1062. https://doi.org/10.1016/j.immuni.2013.03.010.
27. Schoenen H, Bodendorfer B, Hitchens K, Manzanero S, Werninghaus K, Nimmerjahn F, Agger EM, Stenger S, Andersen P, Ruland J, Brown GD, Wells C, Lang R. 2010. Cutting edge: Mincle is essential for recognition and adjuvanticity of the mycobacterial cord factor and its synthetic analog trehalose-dibehenate. J Immunol 184:2756–2760. https://doi.org/10.4049/jimmunol.0904013.
28. Shenderov K, Barber DL, Mayer-Barber KD, Gurcha SS, Jankovic D, Feng CG, Oland S, Hieny S, Caspar P, Yamasaki S, Lin X, Ting JP, Trinchieri G, Besra GS, Cerundolo V, Sher A. 2013. Cord factor and peptidoglycan recapitulate the Th17-promoting adjuvant activity of mycobacteria through mincle/CARD9 signaling and the inflammasome. J Immunol 190:5722–5730. https://doi.org/10.4049/jimmunol.1203343.
29. Portevin D, Gagneux S, Comas I, Young D. 2011. Human macrophage responses to clinical isolates from the Mycobacterium tuberculosis complex discriminate between ancient and modern lineages. PLoS Pathog 7:e1001307. https://doi.org/10.1371/journal.ppat.1001307.
30. Cardoso FLL, Antas PRZ, Milagres AS, Geluk A, Franken KLMC, Oliveira EB, Teixeira HC, Nogueira SA, Sarno EN, Klatser P, Ottenhoff THM, Sampaio EP. 2002. T-cell responses to the Mycobacterium tuberculosis-specific antigen ESAT-6 in Brazilian tuberculosis patients. Infect Immun 70:6707–6714. https://doi.org/10.1128/IAI.70.12.6707-6714.2002.
31. Mustafa AS, Amoudy HA, Wiker HG, Abal AT, Ravn P, Oftung F, Andersen P. 1998. Comparison of antigen-specific T-cell responses of tuberculosis patients using complex or single antigens of Mycobacterium tuberculosis. Scand J Immunol 48:535–543. https://doi.org/10.1046/j.1365-3083.1998.00419.x.
32. De Keyzer J, Van Der Does C, Driessen AJ. 2002. Kinetic analysis of the translocation of fluorescent precursor proteins into Escherichia coli membrane vesicles. J Biol Chem 277:46059–46065. https://doi.org/10.1074/jbc.M208449200.
33. Yarwood JM, Schlievert PM. 2000. Oxygen and carbon dioxide regulation of toxic shock syndrome toxin 1 production by Staphylococcus aureus MN8. J Clin Microbiol 38:1797–1803.
34. Srivastava S, Ernst JD. 2013. Cutting edge: direct recognition of infected cells by CD4 T cells is required for control of intracellular Mycobacterium tuberculosis in vivo. J Immunol 191:1016–1020. https://doi.org/10.4049/jimmunol.1301236.
35. Ernst JD, Cornelius A, Desvignes L, Tavs J, Norris BA. 2018. Limited antimycobacterial efficacy of epitope peptide administration despite enhanced antigen-specific CD4 T-cell activation. J Infect Dis 218:1653–1662. https://doi.org/10.1093/infdis/jiy142.
36. Kauffman KD, Sallin MA, Sakai S, Kamenyeva O, Kabat J, Weiner D, Sutphin M, Schimel D, Via L, Barry CE, III, Wilder-Kofie T, Moore I, Moore R, Barber DL. 2018. Defective positioning in granulomas but not lung-homing limits CD4 T-cell interactions with Mycobacterium tuberculosis-infected macrophages in rhesus macaques. Mucosal Immunol 11:462–473. https://doi.org/10.1038/mi.2017.60.
37. Kruh-Garcia NA, Wolfe LM, Chaisson LH, Worodria WO, Nahid P, Schorey JS, Davis JL, Dobos KM. 2014. Detection of Mycobacterium tuberculosis peptides in the exosomes of patients with active and latent M. tuberculosis infection using MRM-MS. PLoS One 9:e103811. https://doi.org/10.1371/journal.pone.0103811.
38. Smith VL, Cheng Y, Bryant BR, Schorey JS. 2017. Exosomes function in antigen presentation during an in vivo Mycobacterium tuberculosis infection. Sci Rep 7:43578. https://doi.org/10.1038/srep43578.
39. Kuo CJ, Ptak CP, Hsieh CL, Akey BL, Chang YF. 2013. Elastin, a novel extracellular matrix protein adhering to mycobacterial antigen 85 complex. J Biol Chem 288:3886–3896. https://doi.org/10.1074/jbc.M112.415679.
40. Tsujimura Y, Inada H, Yoneda M, Fujita T, Matsuo K, Yasutomi Y. 2014. Effects of mycobacteria major secretion protein, Ag85B, on allergic inflammation in the lung. PLoS One 9:e106807. https://doi.org/10.1371/journal.pone.0106807.
41. Volkman HE, Pozos TC, Zheng J, Davis JM, Rawls JF, Ramakrishnan L. 2010. Tuberculous granuloma induction via interaction of a bacterial secreted protein with host epithelium. Science 327:466–469. https://doi.org/10.1126/science.1179663.
42. National Research Council. 2011. Guide for the care and use of laboratory animals, 8th ed. National Academies Press, Washington, DC.
43. Copin R, Wang X, Louie E, Escuyer V, Coscolla M, Gagneux S, Palmer GH, Ernst JD. 2016. Within host evolution selects for a dominant genotype of Mycobacterium tuberculosis while T cells increase pathogen genetic diversity. PLoS Pathog 12:e1006111. https://doi.org/10.1371/journal.ppat.1006111.
44. Wiens KE, Ernst JD. 2016. The mechanism for type I interferon induction by Mycobacterium tuberculosis is bacterial strain-dependent. PLoS Pathog 12:e1005809. https://doi.org/10.1371/journal.ppat.1005809.
45. Wiens KE, Ernst JD. 2016. Type I interferon is pathogenic during chronic Mycobacterium africanum infection. J Infect Dis 214:1893–1896. https://doi.org/10.1093/infdis/jiw519.
46. de Carvalho LP, Fischer SM, Marrero J, Nathan C, Ehrt S, Rhee KY. 2010. Metabolomics of Mycobacterium tuberculosis reveals compartmentalized co-catabolism of carbon substrates. Chem Biol 17:1122–1131. https://doi.org/10.1016/j.chembiol.2010.08.009.
47. Wolf AJ, Linas B, Trevejo-Nunez GJ, Kincaid E, Tamura T, Takatsu K, Ernst JD. 2007. Mycobacterium tuberculosis infects dendritic cells with high frequency and impairs their function in vivo. J Immunol 179:2509–2519. https://doi.org/10.4049/jimmunol.179.4.2509.